Anisotropy of the critical current in MgB_2 tapes made of high energy milled precursor powder

2010 Supercond. Sci. Technol. 23 065011

(http://iopscience.iop.org/0953-2048/23/6/065011)

Supercond. Sci. Technol. **23** (2010) 065011 (6pp) doi:10.1088/0953-2048/23/6/065011

Anisotropy of the critical current in MgB_2 tapes made of high energy milled precursor powder

W Häßler[1], P Kovac[2], M Eisterer[3], A B Abrahamsen[4], M Herrmann[1], C Rodig[1], K Nenkov[1], B Holzapfel[1], T Melisek[2], M Kulich[2], M v Zimmermann[5], J Bednarcik[5] and J C Grivel[4]

[1] Institute for Metallic Materials, Leibniz-Institute for Solid State and Materials Research (IFW), Dresden, Germany
[2] Institute of Electrical Engineering, Slovak Academy of Sciences, Bratislava, Slovakia
[3] Atomic Institute, Vienna University of Technology, Austria
[4] Materials Research Division, Risø-DTU, Roskilde, Denmark
[5] Hamburger Synchrotronstrahlungslabor HASYLAB at Deutsches Elektronen-Synchrotron DESY, Hamburg, Germany

E-mail: w.haessler@ifw-dresden.de

Received 4 February 2010, in final form 15 March 2010
Published 4 May 2010
Online at stacks.iop.org/SUST/23/065011

Abstract
For applications of MgB_2 wires or tapes, high critical currents in high magnetic fields are essential. By using tapes in superconducting coils the anisotropic behaviour of the critical current, i.e. the dependence on the direction of the external field in relation to the tape surface, has to be taken into account.

The anisotropy of MgB_2 tapes with mechanically alloyed (MA) precursor powder and different sheath materials which can be much higher than the intrinsic anisotropy is discussed. Furthermore tapes with pure and C doped MA-MgB_2 precursor are compared. Tapes with a hard Fe-sheath and undoped precursor show a high extrinsic anisotropy of the critical current density which can be reduced considerably by carbon doping. A texture of the MgB_2 phase in the tape filaments introduced by flat rolling was observed by synchrotron x-ray diffraction. Using this texture information the observed macroscopic I_c-anisotropy of the tapes can be explained by calculations based on the percolation model.

(Some figures in this article are in colour only in the electronic version)

1. Introduction

An important point in the characterization of the electrical properties (critical fields and currents) of MgB_2 tapes is their anisotropy in relation to the direction of the external magnetic field. Usually mostly the properties in parallel field are presented in the literature. But the properties in both field directions are essential for applications.

MgB_2 is a two-band superconductor with anisotropic properties, such as the upper critical field B_{c2}. In undoped bulk samples B_{c2} is about 14 T in a parallel field (with respect to the boron planes spanned by the *ab*-plane of the hexagonal unit cell) and about 3 T in a perpendicular field, so the intrinsic anisotropy, γ, is close to 5 [1]). The first authors to mention the anisotropy of the critical current I_c of MgB_2 tapes were Kumakura *et al* [2]. Before that, Grasso *et al* [3] had drawn attention to the effect of texture on the magnetoresistive properties of MgB_2 tapes. They found an anisotropy in the irreversibility lines of *ex situ* monofilamentary tapes with Ni-sheath. It was discussed in relation to partial MgB_2 grain texturing by cold rolling. Kovac *et al* [4] reported about the I_c-anisotropy in monofilamentary tapes with different sheath materials. The highest anisotropy value of $I_{cpar}/I_{cperp} = 10$ at 10 T was found in *in situ* tapes with an Fe-sheath. This was explained by the texturing of Mg particles during flat rolling of the wires. The texture of MgB_2 formed during final annealing is determined by this Mg texture. Kovac *et al* [5] also processed mechanically alloyed precursor powder in different sheath materials. The largest anisotropy value of 10 at 8 T was found here at tapes with a Ti-sheath.

Also Beilin [6] came in principle to similar results. Rolled tapes exhibit a clear increase in the intensity of (001) peaks, which depends on the sheath material (hardness ...) and the rolling strain during deformation. Lezza [7] has found a texture gradient across the filament diameter. The texture is increasing from the filament centre to the interface to the sheath. Anisotropy values of $I_{cpar}/I_{cperp} = 30$ at 8 T were announced. Serrano *et al* [8] have measured the angular dependence of the critical current density of undoped and SiC doped MgB_2 tapes. They have found that the anisotropy value increased for larger aspect ratios.

After publishing high critical current of tapes with carbon doped MA precursor densities in parallel field [9, 10] we are now going to present experimental results about the critical current anisotropy of these tapes. In addition, we want to give an explanation of this anisotropy in the framework of the percolation model [1] based on texture measurements.

2. Experimental details and simulations

Powders of magnesium (Goodfellow, 99.8%, <250 μm), amorphous boron (Starck, 95%–97%, < 1 μm), and nanostructured carbon (SGL Carbon Werk Ringsdorf, 99.999%) in different concentrations were used. Powder storage and processing were done in a glove box under Ar atmosphere. A partially reacted, nanocrystalline precursor powder with enhanced reactivity was obtained by mechanical alloying using a ball mill Retsch PM 4000 with tungsten carbide milling tools for 50 h at 250 rpm under Ar atmosphere. The technique of mechanical alloying has been shown to be very effective in the preparation of sophisticated precursors [11]. In order to reduce the grain size and enhance the reactivity of the carbon, it was premilled before it was added to the initial weight. Further details are described elsewhere [12]. Using undoped and doped MA precursor powder, monofilamentary tapes were prepared by the powder-in-tube (PIT) method. The powder was filled into Fe tubes and CuNi/Nb double tubes and deformed by swaging and rolling into tapes with filling factors of 18%–22%. Typical dimensions of the tapes are 4.4×0.24 mm^2. Interstage annealing was applied at 500 °C/1 h in Ar atmosphere to reduce work hardening of the sheath. The subsequent final heat treatment was carried out at a temperature of 600 °C in Ar atmosphere (dwell time 3 h), the tapes were wrapped into oxygen getter foil. Additionally a 19-filamentary wire and tape were prepared with undoped precursor in a Fe-sheath (wire Ø 1.5 mm, tape 4.4×0.36 mm^2).

The texture of tapes with Fe-sheath was characterized by measuring the rocking curves of the MgB_2(002) reflection using high energy synchrotron x-ray diffraction of photons with $E = 77.5$ keV at the BW5 beamline in HASYLAB. The high penetration in Fe of the high energy photons allows scattering in transmission mode and the diffraction patterns from the samples were collected on a two-dimensional image plate. A Pb absorber ring was used to damp the strongest reflection from the Fe-sheath material, whereby saturation of the detector was avoided and the quality of the diffraction pattern from the superconductor was improved considerably [13].

The critical temperature was determined by temperature and magnetic field dependent resistance measurements using a physical property measurement system (Quantum Design). The transition width T_c and the critical field B_{c2} and the irreversibility field B_{irr} were determined using the 90% and 10% criteria of the resistance at $T_{c,onset}$. T_c is reported as the temperature at which the resistance dropped to 50% of the resistance at $T_{c,onset}$.

Transport J_c of the tapes was determined in liquid helium (4.2 K) by the standard four-probe method using the 1 μV cm^{-1} electric field criterion. The critical currents were measured in parallel and perpendicular magnetic field orientation in an external field of $\mu_0 H = 3.0$–8.0 T and also at constant fields between 5.5 and 8 T with variable field direction.

The critical currents were simulated numerically by a percolation model for weakly textured media [14]. The intrinsic J_c-anisotropy was modelled by the anisotropic scaling approach proposed by Blatter *et al* [15]. The resulting distribution function of J_c is strongly altered by weak texture and depends, in contrast to untextured materials [1], on the orientation of the tape with respect to the applied magnetic field. We assumed uni-axial texture, with a Gaussian-like exponential distribution (at fixed azimuthal angle), i.e. $\propto \exp(-\alpha^2/2\alpha_t^2)$, where α denotes the angle to the preferred grain orientation (perpendicular to the tape) and α_t characterizes the degree of texture: α_t is zero for perfect texture and infinite in untextured materials (in contrast to a true Gaussian distribution, it is not the standard deviation of the distribution function). We assumed planar defects (e.g. grain boundaries) without any preferential orientation as dominant pinning centres. The model contains five *a priori* unknown parameters: I_{c0}, B_{c2}, γ, α_t, and p_c. I_{c0} is a constant prefactor, which represents the pinning strength and the connectivity [1, 16]. p_c denotes the percolation threshold, which is defined as the minimum fraction of superconducting grains for zero resistivity. Since it is not possible to obtain all five parameters by fitting the experimental data, p_c was fixed at 0.25 [1, 17]. We assumed the experimental value $\alpha_t = 29.3°$ of the carbon doped tape for both samples (see below). The remaining three parameters were chosen to fit the experimental data of $J_c(B)$ in the two main orientations simultaneously. The angular dependence of the critical currents was then calculated with the same parameters.

3. Results and discussions

In figure 1 the cross-sections of a typical monofilamentary and a multifilamentary (19 filaments) tape are shown. Most of the investigations were done on monofilamentary samples, a comparison to multifilamentary tapes is given at the end of this section.

At filaments from which the metallic sheath (Fe) had been stripped off the resistance was measured in relation to the temperature, magnetic field, and angle between tape normal and field. A critical temperature T_c of 36.3 K ($\Delta T_c = 1.2$ K) was measured at the undoped tape. The upper

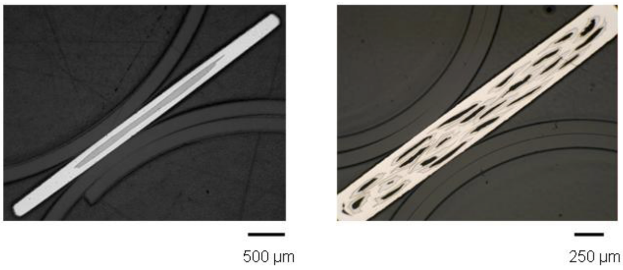

Figure 1. Cross-section of a monofilamentary tape in Fe-sheath and a 19-filamentary tape in CuNi/Nb-sheath.

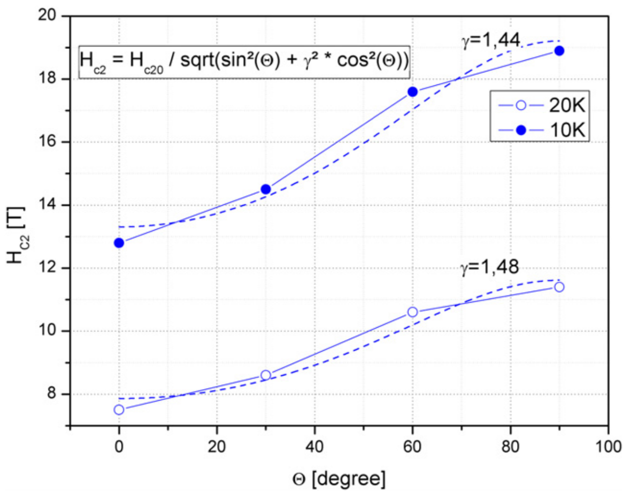

Figure 2. Upper critical field H_{c2} of a tape filament (undoped precursor) as a function of the angle between the tape normal and the magnetic field (90° corresponds to $H_{||}$), as obtained from resistance measurements $R(T, B, \Theta)$ (values at 10 K were extrapolated). The dotted line graphs refer to the prediction of anisotropic Ginzburg–Landau theory.

critical field H_{c2} of an undoped sample evaluated from these $R(T, B, \Theta)$ data is shown in figure 2. An anisotropy value $\gamma_{macro} = H_{c2par}/H_{c2perp}$ of 1.44 and 1.48 was obtained, where H_{c2par} and H_{c2perp} denote the macroscopic upper critical field in parallel and perpendicular field orientations. The angular dependence of H_{c2} does not obey the formula $H_{c2} = H_{c2par}/\text{sqrt}(\sin^2(\Theta) + \gamma^{2*}\cos^2(\Theta))$ predicted by the anisotropic Ginzburg–Landau theory [18] (dotted lines in figure 2), because γ_{macro} does not directly reflect the intrinsic anisotropy. This is evident in untextured MgB_2, where γ_{macro} is unity despite the much larger intrinsic γ. The observed upper critical field anisotropy indicates that the texture is quite significant, since only 2–3% of superconducting grains are needed for reducing the resistivity to 90%. (This estimate is based on a percolation threshold of 0.25.) This means that the number of grains oriented with their boron plane perpendicular to the tape must be extremely small, which is consistent with the α_t found in the synchrotron measurements.

More or less the same values ($\gamma_{macro} \approx 1.5$) were measured for a filament of a C doped tape ($MgB_{1.9}C_{0.13}$). The critical temperature was reduced by carbon doping: $T_c = 31.5$ K ($\Delta T_c = 1.9$ K).

Now we come to the main point of this paper: the anisotropy of the transport critical current density in relation to the field direction. Monofilamentary tapes with undoped MA precursor are characterized by high critical current densities J_c of 10^4 A cm^{-2} at 10–12 T in a parallel field at 4.2 K [10]. Tapes with carbon doped precursor have a J_c of 10^4 A cm^{-2} at higher fields of 14–16 T (depending on deformation technology, annealing temperature, and sheath material) at parallel field and 4.2 K.

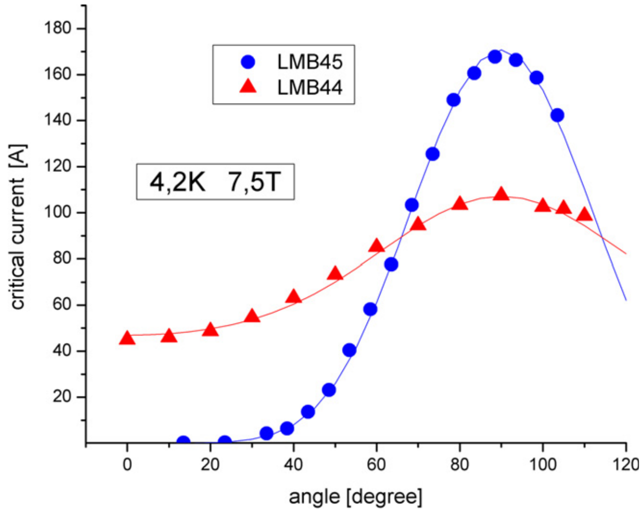

Figure 3. Critical current I_c at 4.2 K and 7.5 T as a function of the field orientation angle of tapes with undoped and nano-carbon doped MA precursor (doping concentration $x = 0.13$ in $Mg(C_xB_{2-x})$). Good agreement between calculated (line graphs) and experimental data is obtained.

As the first point the J_c-anisotropy of Fe-sheathed monofilamentary tapes with undoped and nano-carbon doped precursor should be at the focus. In figure 3 the critical current of an undoped and doped ($x = 0.13$ in $Mg(C_xB_{2-x})$) tape is shown as a function of the angle between the tape normal and the field direction at a fixed field value of 7.5 T at 4.2 K (90° corresponds to the parallel field direction). It can be seen that the difference of critical currents in parallel and perpendicular fields is very high in the undoped tape, the anisotropy value ($k_a = I_{cpar}/I_{cperp}$) is about 500. Carbon doping results in a remarkable decrease of this anisotropy ($k_a \approx 2$), since partial substitution of boron by carbon reduces the intrinsic anisotropy γ and enhances B_{c2} [1, 19–21].

The field dependence of J_c in undoped and doped iron sheathed tapes is shown in figure 4(a). A huge difference between the parallel and perpendicular field orientation is found, especially in the undoped sample. The anisotropy in the field dependence of J_c is decreased considerably by carbon doping.

Figure 4(b) shows the I_c-anisotropy factor k_a (quotient of I_{cpar} and I_{cperp}) versus the external field. One can see that k_a strongly increases with field. An unexpected high extrinsic anisotropy was found at tapes with undoped precursor, i.e. anisotropy factors of higher than 100 in high fields were found. At 8 T a value of $k_a > 10^3$ was measured. These high values are not influenced by the precision of low critical current measurement ($I_c < 0.1$ A, *regular I–V curve*) and are even smaller than expected from the simulations. In comparison, the I_c-anisotropy is much lower ($k_a = 2.5$) in the

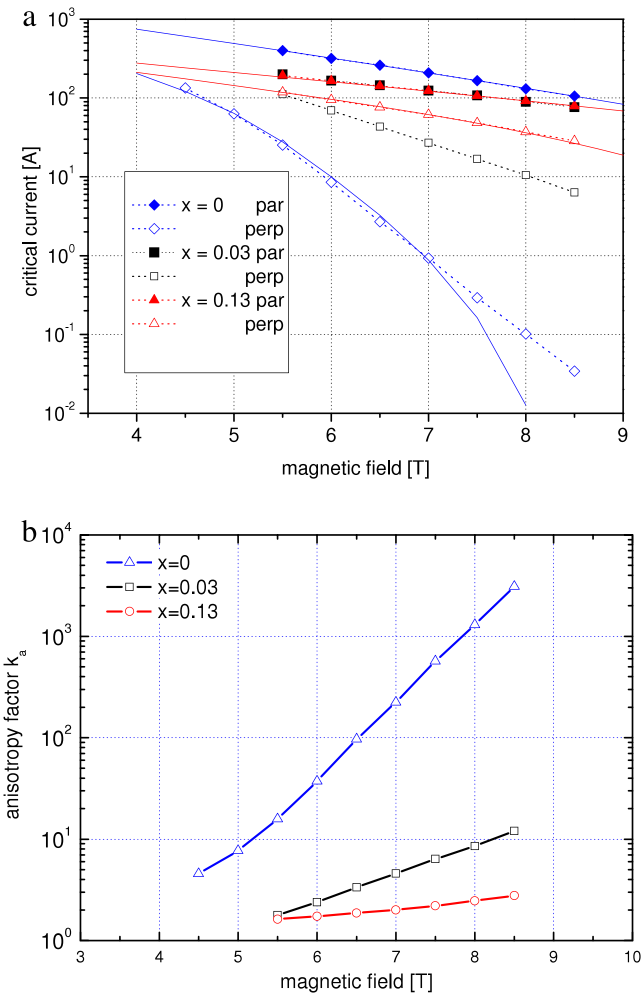

Figure 4. Critical currents measured for tapes with Fe-sheath and undoped or carbon doped MA precursor ($x = 0.03$ and 0.13). Solid lines were calculated numerically. (b) Anisotropy factor of the critical current density measured at tapes with Fe-sheath and undoped or carbon doped MA precursor ($x = 0.03$ and 0.13).

carbon doped sample (0.13%C), which is a consequence of its smaller intrinsic anisotropy.

Following the discussion in the literature that the reason for the anisotropic behaviour of the critical currents in general can be found in the texture of the MgB_2 grains, which are partially aligned with the normal of the tape, we have investigated the texture of some tapes by x-ray. Synchrotron measurements have shown that the initial rolling of the Mg and B powder inside the Fe-sheathed tape causes an Mg grain alignment, which is subsequently transferred to the MgB_2 grains during the final annealing [13]. Figure 5(a) shows how a partial alignment of the c-axis of the MgB_2 grains can be determined by synchrotron x-ray diffraction from the c-axis (002) reciprocal scattering vectors, which are distributed with two poles on a sphere. Scattering from the (002) reflection of a grain is obtained when the reciprocal vector $\boldsymbol{q}$ of a crystallographic plane in the grain is equal to the difference between the incoming wavevector $\boldsymbol{k}_i$ and the scattered wavevector $\boldsymbol{k}_f$. Thus a small fraction of the (002) reflections on the sphere is observed on the detector at a fixed angle α between the preferred c-axis texture and the incoming x-ray beam along $\boldsymbol{k}_i$. The use of high energy photons with $\lambda = 0.159\,93$ Å results in small scattering angles $2\theta_{(002)} = 2\arcsin(\lambda/2d) = 5.206°$, since $d_{MgB_2(002)} = 1.7608$ Å, and the $\boldsymbol{q}$ vectors which can fulfil the scattering condition are all close to perpendicular to the incoming x-ray beam. The integrated intensity of the (002) reflection as a function of the rocking angle is measured by exposing a two-dimensional detector while the rocking angle is moved continuously in small intervals of 2°–5°. Figures 5(b) and (c) show how the (002) reflection becomes visible as the rocking angle is increased from $\alpha = 25°$ to 65°. The total integrated intensity of the (002) reflection is determined by first integrating the two-dimensional intensity distribution over the azimuthal angle and fitting a Gaussian peak to the radial intensity distribution corresponding to the (002) reflection.

Figure 6 shows the obtained MgB_2(002) and (100) integrated intensity I as a function of the rocking angle and I is given by

$$I_{(hkl)} \propto V_0 \sigma_{(hkl)}(\alpha) I_0 \exp(-\mu_{Fe} l_{Fe}) \tag{1}$$

where V_0 is the illuminated sample volume, $\sigma_{(hkl)}(\alpha)$ is the scattering cross-section of the $MgB_2(hkl)$ reflection at a specific rocking angle α, I_0 is the incoming x-ray intensity, which is damped by the Fe mass attenuation coefficient $\mu_{Fe,E=77.5\text{ keV}} = 5.29\text{ cm}^{-1}$ along the path in the Fe-sheath l_{Fe}. The inset of figure 6 shows that the absorption path $l_{Fe} = t_{Fe}/\cos(\alpha)$ is related to the thickness of the Fe-sheath material $t_{Fe} = 160$–$220\ \mu$m, which includes both the incoming and diffracted path since the influence of the small scattering angle $2\theta_{(002)}$ is neglected. The illuminated volume of MgB_2 $V_0 = t_{SC} d_{beam}/\cos(\alpha)$ is related to the MgB_2 layer thickness $t_{SC} = 60$–$100\ \mu$m and to the beamsize $d_{beam} = 1.0$ mm until the Fe edges of the tape cut the incoming beam at $\alpha > \arccos(d_{beam}/L_{SC}) \sim 66°$ since $L_{SC} = 2.5$ mm. Thus the MgB_2(002) intensity is first expected to increase as the tape normal is rotated away from the incident beam and then decrease sharply at around $\alpha = 90°$. The MgB_2(100) is, on the contrary, expected to decrease around $\alpha = 0°$, then increase as the illuminated volume increases and finally decrease due to the cutting by the Fe edges.

A Gaussian texture distribution $\sigma_{(002)}(\alpha') \sim \exp(\alpha'^2/(2\alpha_t^2))$, where α_t is the width of the texture distribution from the preferred orientation, has been fitted to the MgB_2(002) intensity in the range where the incoming beam is not cut. A texture width of $\alpha_t = 27.8 \pm 2.2°$ was found for the undoped tape whereas the $x = 0.13$ carbon doped tape had $\alpha_t = 29.3 \pm 0.27°$. The texture is the same in both tapes within experimental accuracy. Figure 6 shows a model integration of the assumed Gaussian texture distribution with $\alpha = 27.8°$ including the absorption and illuminated volume corrections, and good agreement is obtained in the un-cut region $|\alpha| < 66°$.

The numerical calculations with the percolation model for weakly textured media (solid lines) nicely describe the data at high currents with $I_{c0} = 2840/860$ A, $B_{c2} = 23.2/20.5$ T, and $\gamma = 4.05/1.8$ for the undoped/doped tape. The disagreement at low currents (<1 A) (figure 4(a)) might be caused by small normal currents driven by the finite voltage (1 μV cm^{-1}) in transport measurements. Such currents were not accounted

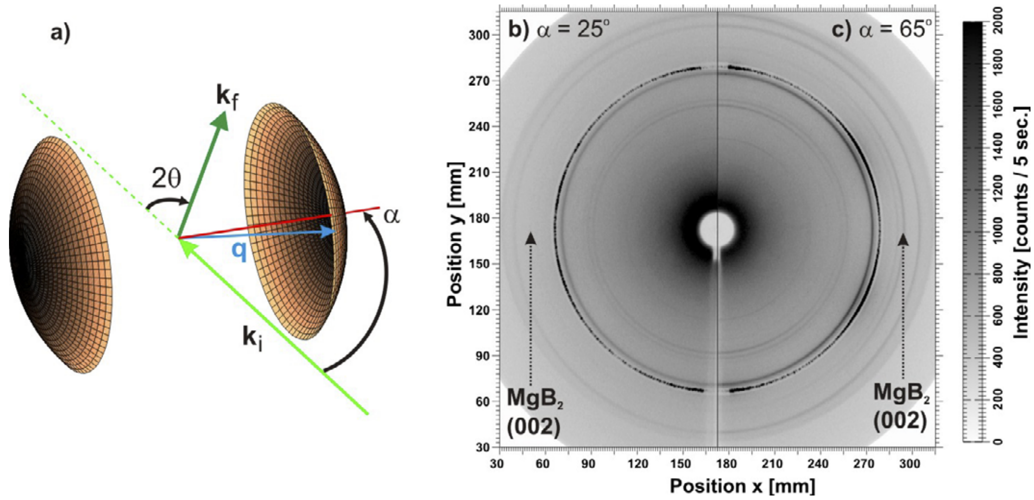

Figure 5. (a) The contour surface shows an assumed Gaussian angular distribution of the reciprocal (002) vector of the MgB_2 grains in a tape, where the *c*-axis has been aligned to the normal vector of the tape by rolling. The distribution is centred around the tape normal and the width is given by α_t whereby $f(\alpha) \sim \exp(-\alpha'^2/(2\alpha_t^2))$. Scattering from a MgB_2(002) grain reflection is obtained when the reciprocal $\boldsymbol{q}$ vector is equal to the difference between the incoming $\boldsymbol{k}_i$ and the scattered wavevector $\boldsymbol{k}_f$, $\boldsymbol{\kappa} = \boldsymbol{k}_f - \boldsymbol{k}_i = \boldsymbol{q}$. Thus sections of the texture distribution can be measured by rotating the angle α between the incoming wavevector $\boldsymbol{k}_i$ and the tape normal while the diffraction pattern is collected on a two-dimensional detector. (b) and (c) shows half of the diffraction pattern of the MgB_2 tape when the tape normal is rotated by $\alpha = 25°$ and $\alpha = 65°$, respectively. The partial Debye–Scherrer ring of the MgB_2(002) reflection appears as the tape normal is rotated away from the direction of the incoming beam.

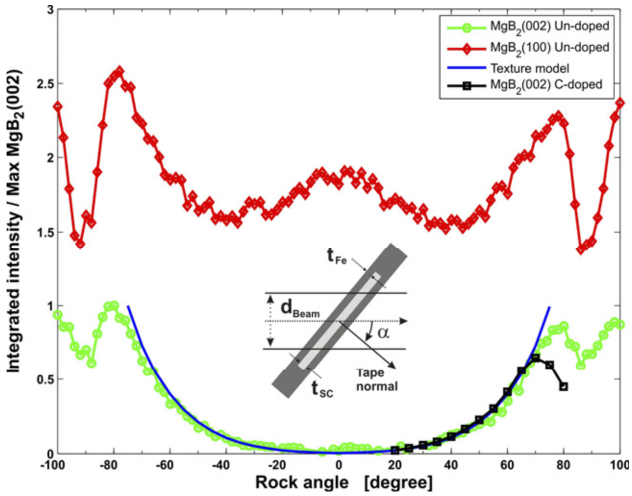

Figure 6. Rocking curve of MgB_2(100) and MgB_2(002) reflections for the undoped sample as a function of the angle α between the incident synchrotron beam and the tape normal as shown by the inset. The decrease of the intensity for $\alpha > 66°$ is caused by the Fe edges of the tape, which are cutting the incoming beam. The MgB_2(002) intensity has been fitted by the Gaussian texture distribution and a texture width $\alpha_t = 27.8 \pm 2.2°$ was found for the undoped sample, whereas the doped sample showed a width of $\alpha_t = 29.3 \pm 0.27°$. The rocking curve of the doped sample has been scaled to show the similarity to the undoped sample.

for in the percolation model and may connect otherwise disconnected superconducting clusters, thus enabling much larger additional currents than expected from the voltage and the normal state resistivity. An alternative explanation lies in texture gradients [7]. The smaller I_{c0} in the doped tape is a consequence of carbon substitution [1, 19–21] but might also indicate worse connectivity [1, 16, 21, 22]. The anisotropy parameter γ is in good agreement with expectations based on its transition temperature [1]. The upper critical field of the doped tape on the other hand is surprising at first glance, since reference measurements on bulk samples [23] would suggest an upper critical field of around 30 T at 4.2 K. However, the irreversibility field in perpendicular orientation is lower by a factor of 0.7 in the tape than in the filaments at low temperatures. Since the irreversibility field is expected to be proportional to the upper critical field, it is reasonable to assume that the upper critical fields differ by the same factor, which confirms the estimate of B_{c2} (20.5 T). We also note that B_{c2} and γ are close to the values reported for a carbon doped single crystal with a T_c of 30.5 K (doped tape: 29.5 K). The B_{c2} of the undoped tape, on the other hand, is slightly too large in relation to the corresponding value of the doped sample, but the reason for this has been unclear up to now.

Figure 7 presents k_a values for tapes with a CuNi/Nb double sheath. Two main points attract attention. First, the anisotropy is decreased remarkably by carbon doping. Second, the anisotropy of the Fe-sheathed tape with undoped precursor is much more pronounced than in the tape with a CuNi/Nb double sheath. In the tapes with a carbon doped precursor, the anisotropy value is reduced and similar in both types of tapes. Due to the reduced anisotropy of doped tapes, they are characterized by high J_c values in parallel fields and in perpendicular fields. At a field of 8 T J_c values of 1×10^5 A cm^{-2} in a parallel field and 4.5×10^4 A cm^{-2} in a perpendicular field could be measured at these tapes. While for undoped and iron sheathed tape $k_a > 10^3$ is measured, CuNi/Nb-sheathed tape has $k_a \approx 10$. This difference (two orders of magnitude) can be attributed to the mechanical strength of the used sheath materials possibly resulting in better texture (smaller α_t).

The critical current anisotropy of multicore (19 filaments) CuNi/Nb-sheathed tape with undoped precursor was also

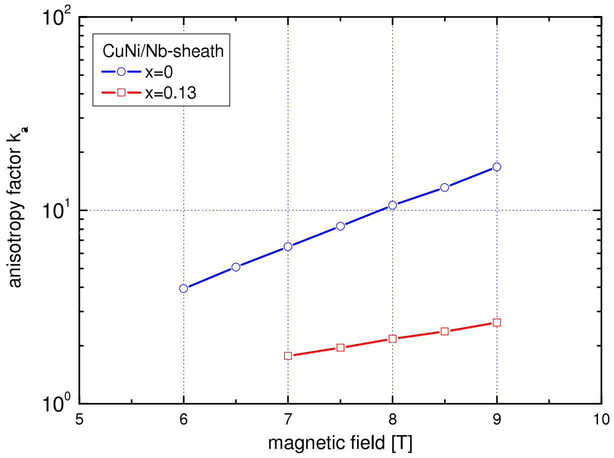

Figure 7. Anisotropy factor of the critical current density k_a measured at tapes with CuNi/Nb double sheath and undoped or carbon doped MA precursor ($x = 0.13$).

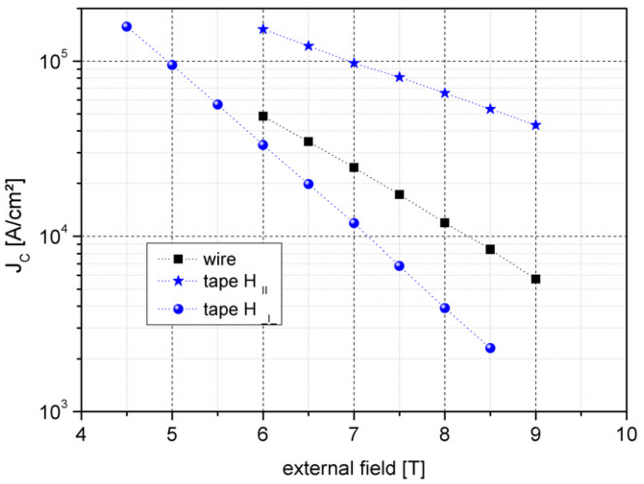

Figure 8. Comparison of the critical current density of multifilamentary tape and wire (19 filaments, CuNi/Nb-sheath).

measured. Figure 8 shows the comparison of $J_c(B)$ dependence for the tape and the wire. The critical current of the isotropic wire (1.5 mm) in parallel field was considerably increased by flat rolling to a tape (4.4 mm × 0.35 mm). On the other hand, J_{cperp} is slightly decreased, which is expected from texturing [14]. A k_a-value of 16 was estimated for the tape sample at 8 T, which is lower than for a single-core tape, see figure 4. The aspect ratio for the monofilamentary tape is about 30, for a 19-filamentary one it was about $5 \cdots 10$ (inhomogeneous filament shape).

4. Summary

A large anisotropy of the transport critical current of MgB_2-tapes in an external magnetic field was observed. As a first experimental result it was proved that the angle dependence of the resistance in constant field is described by the intrinsic anisotropy. An unexpectedly high extrinsic anisotropy was found in the critical current density of Fe-sheathed tapes, i.e. anisotropy factors of higher than 100 in high fields were measured at tapes with undoped precursor. This anisotropy is influenced by the used sheath material (Fe or CuNi/Nb). The anisotropy is remarkably decreased by carbon doping of the precursor powder, for such tapes only anisotropy factors of lower than 3 at $B < 9$ T were measured.

As the main reason for the anisotropic behaviour of J_c the texture of the filaments has already been discussed in the literature. Rolling of wires to tapes gives a texture in the Mg phase which is transferred to the MgB_2 crystallites during annealing. The texture of filaments was characterized in Fe-sheathed tapes by measuring rocking curves of the MgB_2(002) reflection using high energy synchrotron x-ray diffraction.

A percolation model adopted to nonlinear transport in weakly textured media was successful in describing the field and angular dependence of the critical current density of MgB_2-tapes using the measured texture width.

Acknowledgments

The authors want to thank J Scheiter and K Schröder for technical assistance. This work was supported by the EU-FP6 Specific Targeted Research Project HIPERMAG (STRP 505724-1).

References

[1] Eisterer M 2007 *Supercond. Sci. Technol.* **20** R47
[2] Kumakura K, Matsumoto A, Fujii H, Kitaguchi H and Togano K 2002 *Physica* C **382** 93
[3] Grasso G, Malagoli A, Marre D, Bellingeri E, Braccini V, Roncallo S, Scati N and Siri A S 2002 *Physica* C **378–381** 899
[4] Kovac P, Melisek T and Husek I 2005 *Supercond. Sci. Technol.* **18** L45
[5] Kovac P, Husek I, Dobrocka E, Melisek T, Haessler W and Herrmann M 2008 *Supercond. Sci. Technol.* **21** 015004
[6] Beilin V, Lapides I, Roth M, Dul'kin E, Mojaev E, Gerber A and Riss O 2006 *J. Appl. Phys.* **100** 043903
[7] Lezza P, Gladyshevskii L P, Abächerli V and Flükiger R 2006 *Supercond. Sci. Technol.* **19** 286
[8] Serrano G *et al* 2008 *J. Phys.: Conf. Ser.* **97** 012129
[9] Häßler W, Herrmann M, Rodig C, Schubert M, Nenkov K and Holzapfel B 2008 *Supercond. Sci. Technol.* **21** 062001
[10] Herrmann M, Haessler W, Rodig C, Gruner W, Holzapfel B and Schultz L 2007 *Appl. Phys. Lett.* **91** 082507
[11] Schultz L and Eckert J 1994 Mechanically alloyed glassy metals *Glassy Metals III* ed H Beck and H J Güntherodt (Berlin: Springer) chapter 3, p 69
[12] Gruner W, Herrmann M, Nilsson A, Hermann H, Haessler W and Holzapfel B 2007 *Supercond. Sci. Technol.* **20** 601
[13] Abrahamsen A B, Grivel J-C, Andersen N H, Homeyer J and Saksl K 2007 *IEEE Trans. Appl. Supercond.* **17** 2757
[14] Eisterer M, Häßler W and Kovac P 2009 *Phys. Rev.* B **80** 174516
[15] Blatter G, Geshkenbein V B and Larkin A I 1992 *Phys. Rev. Lett.* **68** 875
[16] Rowell J M 2003 *Supercond. Sci. Technol.* **16** R17
[17] Eisterer M, Emhofer J, Sorta S, Zehetmayer M and Weber H W 2009 *Supercond. Sci. Technol.* **22** 034016
[18] Tilley D R 1965 *Proc. Phys. Soc. Lond.* **86** 289
[19] Masui T, Lee S and Tajima S 2004 *Phys. Rev.* B **70** 024504
[20] Krutzler C, Zehetmayer M, Eisterer M, Weber H W, Zhigadlo N D, Karpinski J and Wisniewski A 2006 *Phys. Rev.* B **74** 144511
[21] Kim J H, Dou S X, Oh S, Jercinovic M, Babic E, Nakane T and Kumakura H 2008 *J. Appl. Phys.* **104** 063911
[22] Eisterer M, Müller R, Schöppl R, Weber H W, Soltanian S and Dou S X 2007 *Supercond. Sci. Technol.* **20** 117
[23] Fuchs G and Kozlova A 2008 private communication